Tunnelling spectra for (d_{x2-y2} + is)-wave superconductors versus tunnelling spectra for (d_{x2-y2} + id_{xy})-wave superconductors

2001 J. Phys.: Condens. Matter 13 1265

(http://iopscience.iop.org/0953-8984/13/6/307)

INSTITUTE OF PHYSICS PUBLISHING JOURNAL OF PHYSICS: CONDENSED MATTER

J. Phys.: Condens. Matter **13** (2001) 1265–1278 www.iop.org/Journals/cm PII: S0953-8984(01)17599-5

Tunnelling spectra for ($d_{x^2-y^2}$ + is)-wave superconductors versus tunnelling spectra for ($d_{x^2-y^2}$ + id_{xy})-wave superconductors

N Stefanakis

Department of Physics, University of Crete, PO Box 2208, GR-71003, Heraklion, Crete, Greece

Received 29 September 2000

Abstract

The tunnelling conductance spectrum of a normal-metal/insulator/singlet superconductor is calculated from the reflection amplitudes using the Blonder–Tinkham–Klapwijk (BTK) formulation. The pairing symmetry of the superconductor is assumed to be $d_{x^2-y^2}$ + is or $d_{x^2-y^2}$ + id_{xy}. It is found that in the ($d_{x^2-y^2}$ + is)-wave case there is a well defined conductance peak in the conductance spectra, in the amplitude of the secondary s-wave component. In the ($d_{x^2-y^2}$ + id_{xy})-wave case the tunnelling conductance has residual values within the gap, due to the formation of bound states. The bound-state energies depend on the angle of the incident quasiparticles, and also on the boundary orientation. On the basis of this observation, an electron-focusing experiment is proposed to probe the ($d_{x^2-y^2}$ + id_{xy})-wave state.

1. Introduction

Two decades ago, Blonder *et al* [1] used the Bogoliubov–de Gennes (BdG) equations to calculate the tunnelling conductance of normal-metal/s-wave superconductor contacts, with a barrier of arbitrary strength between them, in terms of the probability amplitudes of Andreev [2] and normal reflection. In the Andreev reflection process an electron incident on the barrier can be reflected as an electron (normal reflection), reflected as a hole without changing its momentum (Andreev reflection), and it can also be transmitted into the superconductor as an electron-like or hole-like quasiparticle.

Recently the BTK theory was extended by several groups to consider the anisotropy of the pair potential. In d-wave superconductors the pair potential changes sign under a 90° rotation. So under appropriate orientation of the a-axis of the d-wave superconductor the transmitted quasiparticle 'feels' different signs of the pair potential. This results in the formation of bound states within the energy gap, which are detected as peaks in the conductance spectra. In the d-wave superconductor there is a peak at $E = 0$ for a great range of angles of incidence of the incoming electron. This range depends on the surface orientation [3]. In particular, for (110) surfaces the peak exists at $E = 0$ for all angles of incidence, and disappears for the (010) and (100) surfaces.

0953-8984/01/061265+14$30.00

In the presence of another barrier inside the normal metal, additional subgap bound states exist due to multiple Andreev reflections [4, 5]. The same phenomenon occurs in the d-wave superconductor/insulator/d-wave superconductor system. For these systems the quasiparticle current has been examined by several groups [6–8], using BTK formalism with recursive relations for the determination of the probability amplitudes.

There is a competition between different pairing symmetries in the bulk. The coexistence of a subdominant order parameter for the bulk depends on the strength of the secondary-order-parameter attractive interaction relative to the attractive interaction in the dominant pairing channel. When the secondary order parameter is strong enough, a second phase transition occurs at a temperature $T_{c1} < T_c$ which depends on the strength of the secondary order parameter. Numerical results show that when such coexistence is realized, the relative phase of the order parameters is $\pi/2$, leading to a $d_{x^2-y^2}$ + is or $d_{x^2-y^2}$ + id_{xy} pairing state in the bulk. The temperature dependences of the various thermodynamic quantities and transport properties change from power laws to exponentials below T_{c1} [9, 10]. When the secondary order parameter is not strong enough, only the $d_{x^2-y^2}$-wave order parameter appears for the bulk. For (110) surfaces the $d_{x^2-y^2}$-wave order parameter changes sign under reflection at the surface and vanishes at the surface. On the other hand, the s and d_{xy} ones do not change sign and are not affected by the presence of the surface, so there is a possibility of their presence near the surface even when their attractive interaction is not strong enough for them to exist in the bulk [11, 12].

The presence of the secondary order parameter near a surface is manifested in tunnelling spectra as a splitting of the zero-energy conductance peak (ZEP) at low temperatures at zero external field and further non-linear splitting with increasing external field [13]. The field dependence of the splitting of the ZEP in the tunnelling spectra of YBCO has been examined [14, 15]. The observation is consistent with a $d_{x^2-y^2}$ + is surface order parameter or a $d_{x^2-y^2}$ + id_{xy} order parameter.

In this paper we extend the BTK formula to calculate the tunnelling conductance in a normal-metal/insulator/($d_{x^2-y^2}$+is)-wave or ($d_{x^2-y^2}$+id_{xy})-wave superconductor. In particular we find that in the $d_{x^2-y^2}$ + is state the conductance peak remains rigid at the energy of the subdominant (s) order parameter [16, 17]. Also, in the $d_{x^2-y^2}$ + id_{xy} state, there is a plateau region inside the gap due to the formation of bound states at discrete values of the quasiparticle trajectory angle θ, for all junction orientations. In addition, the evolution of the tunnelling conductance with temperature depends on the nature of the subdominant order parameter. These features can be used to distinguish between states with broken time-reversal symmetry.

2. The model for the NS interface

We consider the normal-metal/insulator/superconductor junction shown in figure 1. We choose the y-direction to be parallel to the interface, and the x-direction to be normal to the interface. The insulator is modelled by a delta function, located at $x = 0$, of the form $V\delta(x)$. The temperature is fixed at 0 K.

The motion of quasiparticles in inhomogeneous superconductors is described by the BdG equations

$$\begin{aligned} &\mathcal{H}_e(\boldsymbol{r})u(\boldsymbol{r}) + \int \mathrm{d}\boldsymbol{r}'\ \Delta(\boldsymbol{s},\boldsymbol{x})v(\boldsymbol{r}') = Eu(\boldsymbol{r}) \\ &\int \mathrm{d}\boldsymbol{r}'\ \Delta^*(\boldsymbol{s},\boldsymbol{x})u(\boldsymbol{r}') - \mathcal{H}_e^*(\boldsymbol{r})v(\boldsymbol{r}) = Ev(\boldsymbol{r}) \end{aligned} \tag{1}$$

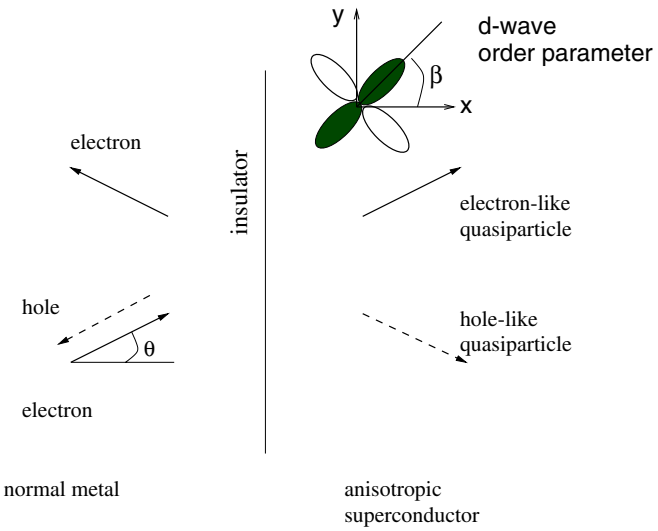

Figure 1. The geometry of the normal-metal/insulator/superconductor interface. The vertical line along the y-axis represents the insulator. The arrows illustrate the transmission and reflection processes at the interface. In this figure, β is the angle between the normal to the interface and the a-axis of the superconductor, and θ is the angle between the incident electron beam and the normal. At the top, the d-wave order parameter is shown.

where the single-particle Hamiltonian is given by

$$\mathcal{H}_e(\boldsymbol{r}) = -\hbar^2\nabla_r^2/2m_e + V(\boldsymbol{r}) - E_F$$

and E is the energy measured from the Fermi energy E_F. $\Delta(\boldsymbol{s}, \boldsymbol{x})$ is the pair potential, after a transformation from the position coordinates $\boldsymbol{r}, \boldsymbol{r}'$ to the centre-of-mass coordinate $\boldsymbol{x} = (\boldsymbol{r} + \boldsymbol{r}')/2$, and the relative vector $\boldsymbol{s} = \boldsymbol{r} - \boldsymbol{r}'$. After Fourier transformation the pair potential depends on the related wave vector $\boldsymbol{k}$, and $\boldsymbol{x}$. In the weak-coupling limit, $\boldsymbol{k}$ is fixed on the Fermi surface ($|\boldsymbol{k}| = k_F$), and only its direction θ is a variable. Also we neglect any spatial variation near the interface, i.e. the pair potential does not depend on $\boldsymbol{x}$. The pair potential has the form

$$\Delta(\boldsymbol{x}, \theta) = \begin{cases} 0 & x < 0 \\ \Delta(\theta) & x > 0 \end{cases} \tag{2}$$

where θ is the angle of the quasiparticle trajectory measured from the x-axis. When a beam of electrons is incident from the normal metal to the insulator, with an angle θ, the general solution of equations (1) is a two-component wave function, which for $x < 0$ is written as

$$\Psi_{\mathrm{I}} = \begin{pmatrix} 1 \\ 0 \end{pmatrix} \mathrm{e}^{\mathrm{i}q_e x\cos\theta} + a\begin{pmatrix} 0 \\ 1 \end{pmatrix} \mathrm{e}^{\mathrm{i}q_h x\cos\theta} + b\begin{pmatrix} 1 \\ 0 \end{pmatrix} \mathrm{e}^{-\mathrm{i}q_e x\cos\theta} \tag{3}$$

while for $x > 0$, the solution is

$$\Psi_{\mathrm{II}} = c\begin{pmatrix} u_+\phi_+ \\ v_+ \end{pmatrix} \mathrm{e}^{\mathrm{i}k_e x\cos\theta} + d\begin{pmatrix} v_-\phi_- \\ u_- \end{pmatrix} \mathrm{e}^{-\mathrm{i}k_h x\cos\theta} \tag{4}$$

where a, b, are the amplitudes for Andreev and normal reflection, and c, d are the amplitudes for transmission into the superconductor as electron-like and hole-like quasiparticles respectively. In the following we assume that $q_e \approx q_h \approx k_e \approx k_h \approx k_F$. The latter approximation is valid within the BCS weak-coupling theory. The BCS coherence factors are given by

$$u_\pm^2 = [1 + \sqrt{E^2 - |\Delta_\pm(\theta)|^2}/E]/2 \tag{5}$$

and

$$v_{\pm}^2 = [1 - \sqrt{E^2 - |\Delta_{\pm}(\theta)|^2}/E]/2. \tag{6}$$

The internal phase arising from the energy gap is given by $\phi_{\pm} = [\Delta_{\pm}(\theta)/|\Delta_{\pm}(\theta)|]$, where $\Delta_{+}(\theta) = \Delta(\theta)$ ($\Delta_{-}(\theta) = \Delta(\pi - \theta)$) is the pair potential experienced by the transmitted electron-like (hole-like) quasiparticle. Using the matching conditions for the wave function at $x = 0$, $\Psi_{\mathrm{I}}(0) = \Psi_{\mathrm{II}}(0)$ and $\Psi'_{\mathrm{II}}(0) - \Psi'_{\mathrm{I}}(0) = (2mV/\hbar^2)\Psi_{\mathrm{I}}(0)$, the magnitudes of the Andreev and normal reflection, $R_a = |a|^2$ and $R_b = |b|^2$, are obtained as [16]

$$R_a = \frac{\sigma_N^2 |n_+|^2}{|1 + (\sigma_N - 1)n_+ n_- \phi_- \phi_+^*|^2} \tag{7}$$

$$R_b = \frac{(1 - \sigma_N)|1 - n_+ n_- \phi_- \phi_+^*|^2}{|1 + (\sigma_N - 1)n_+ n_- \phi_- \phi_+^*|^2} \tag{8}$$

where $n_{\pm} = v_{\pm}/u_{\pm}$. The tunnelling conductance, normalized by that in the normal state, is given by [1]

$$\sigma(E) = \left(\int_{-\pi/2}^{\pi/2} \mathrm{d}\theta\, \overline{\sigma}_{\mathrm{s}}(E, \theta)\right) \Bigg/ \left(\int_{-\pi/2}^{\pi/2} \mathrm{d}\theta\, \sigma_N\right). \tag{9}$$

According to the BTK formula, the conductance of the junction $\overline{\sigma}_{\mathrm{s}}(E, \theta)$ is expressed in terms of the probability amplitudes a and b: $\overline{\sigma}_{\mathrm{s}}(E, \theta) = 1 + R_a - R_b$. The transparency of the junction σ_N is connected to the barrier height V by the relation

$$\sigma_N = \frac{4\cos^2\theta}{Z^2 + 4\cos^2\theta} \tag{10}$$

where $Z = 2mV/\hbar^2 k_F$ denotes the strength of the barrier. In the $Z = 0$ (large-σ_N) limit the interface is regarded as a weak link, showing metallic behaviour, while for large values of Z ($\sigma_N = 0$) the interface becomes insulating.

We consider the following cases:

(a) In the case of a $\mathrm{d}_{x^2-y^2}$-wave superconductor,

$$\Delta(\theta) = \Delta_1(T)\cos[2(\theta - \beta)] \tag{11}$$

where β denotes the angle between the normal to the interface and the x-axis of the crystal. The temperature dependence of the gap follows the usual BCS relation, namely $\Delta_1(T) = \Delta_{\mathrm{d}}\sqrt{1 - T/T_{\mathrm{d}}}$, where T_{d} is the transition temperature.

(b) In the $(\mathrm{d}_{x^2-y^2} + \mathrm{is})$-wave case,

$$\Delta(\theta) = \Delta_1(T)\cos[2(\theta - \beta)] + \mathrm{i}\Delta_2(T) \tag{12}$$

where $\Delta_2(T) = \Delta_{\mathrm{s}}\sqrt{1 - T/T_{\mathrm{s}}}$, and T_{s} is the transition temperature for the s-wave component.

(c) In the $(\mathrm{d}_{x^2-y^2} + \mathrm{id}_{xy})$-wave case,

$$\Delta(\theta) = \Delta_1(T)\cos[2(\theta - \beta)] + \mathrm{i}\Delta_2(T)\sin[2(\theta - \beta)] \tag{13}$$

where the angular form of the secondary component is obtained by the substitution for β in the $\mathrm{d}_{x^2-y^2}$-wave order parameter with $\beta + \pi/4$. $\Delta_2(T) = \Delta_{\mathrm{d}_{xy}}\sqrt{1 - T/T_{\mathrm{d}_{xy}}}$ follows the BCS relation, and $T_{\mathrm{d}_{xy}}$ is the transition temperature for the d_{xy}-wave component.

3. Tunnelling conductance characteristics

In figures 2–4 we plot the tunnelling conductance $\sigma(E)$ as a function of E/Δ_0 for various values of Z, for different orientations (a) $\beta = 0$, (b) $\pi/8$, (c) $\pi/4$. The pairing symmetry of the superconductor is: $d_{x^2-y^2}$-wave symmetry, with $\Delta_d = 0.7\Delta_0$, in figure 2; $(d_{x^2-y^2} + is)$-wave symmetry, with $\Delta_d = 0.7\Delta_0$, $\Delta_s = 0.3\Delta_0$, in figure 3; $(d_{x^2-y^2} + id_{xy})$-wave symmetry, with $\Delta_d = 0.7\Delta_0$, $\Delta_{d_{xy}} = 0.3\Delta_0$ in figure 4. It is clear from these figures that the peaks are narrowed by the increase of Z. In this section the temperature is fixed at 0 K.

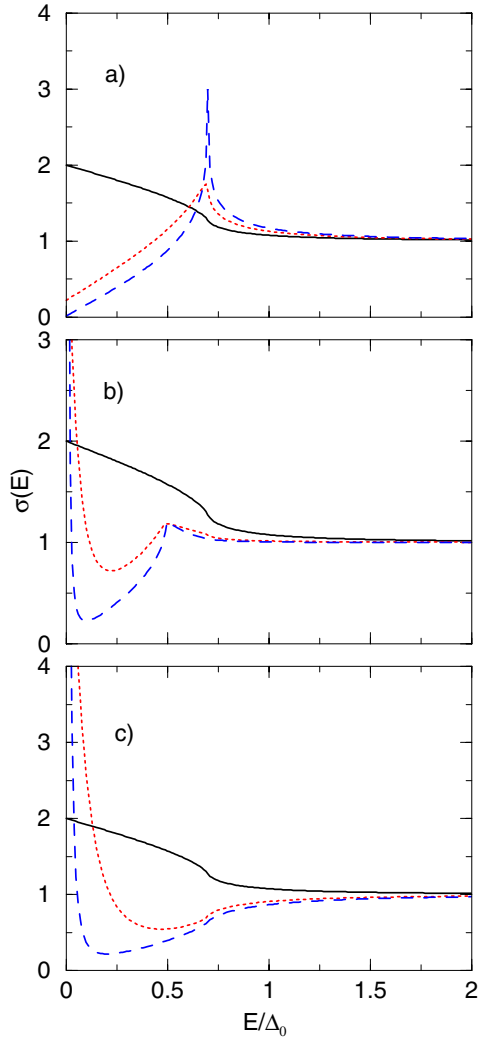

Figure 2. Normalized tunnelling conductance $\sigma(E)$ as a function of E/Δ_0 for $Z = 0$ (solid line), $Z = 2.5$ (dotted line), $Z = 10$ (dashed line), for different orientations (a) $\beta = 0$, (b) $\pi/8$, (c) $\pi/4$. The pairing symmetry of the superconductor is $d_{x^2-y^2}$; $\Delta_d = 0.7\Delta_0$. The temperature is $T = 0$.

For $\beta = 0$, i.e. when the lobes of the dominant d-wave component point towards the junction interface, the position of the conductance peak is near the energy gap Δ_d in all of the above pairing symmetries. This peak mainly arises from the bulk density of states.

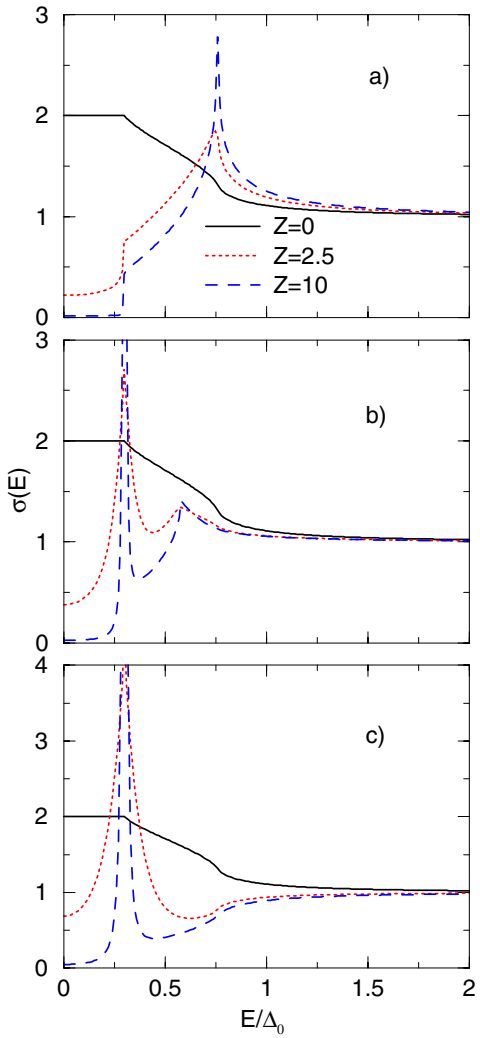

Figure 3. As figure 2, but the pairing symmetry of the superconductor is $d_{x^2-y^2}$+is; $\Delta_d = 0.7\Delta_0$; $\Delta_s = 0.3\Delta_0$.

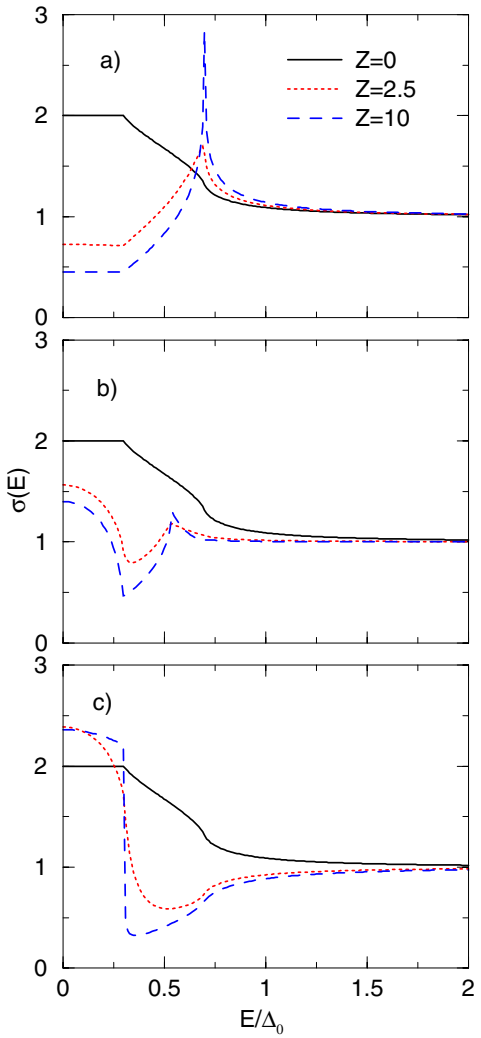

Figure 4. As figure 2, but the pairing symmetry of the superconductor is $d_{x^2-y^2} + id_{xy}$; $\Delta_d = 0.7\Delta_0$; $\Delta_{d_{xy}} = 0.3\Delta_0$.

For $\beta \neq 0$ another peak exists in the conductance spectra, for the $d_{x^2-y^2}$-wave and ($d_{x^2-y^2}$ + is)-wave cases, but its physical origin is different to that found near Δ_d. For the d-wave case this peak exists at $E = 0$ for all of the non-zero values of β, due to the different sign of the pair potential that the transmitted quasiparticles feel. However, the height of the conductance peak (ZEH) depends on the orientation angle β. For a given angle β, the ZEH is proportional to the range of θ-angles for which sign change occurs. This is seen in figure 2(c) for $\beta = \pi/4$ where the ZEH is maximum, since for this orientation the transmitted quasiparticles feel a different sign of the pair potential for all angles $-\pi/2 < \theta < \pi/2$. On the other hand, for $\beta = \pi/8$ in figure 2(b) the range of angles is reduced and the ZEH takes a lower value.

For the ($d_{x^2-y^2}$ + is)-wave case in figure 3, the position of the conductance peak is shifted to the energy $E = \Delta_s$, for all values of β. For each value of β, its height depends on the range

of θ-angles where the transmitted quasiparticles feel a different sign of the pair potential. For $\beta = \pi/4$ the conductance peak, as seen in figure 3(c) at $E = \Delta_s$, has its maximum value, since the transmitted quasiparticles feel the sign change of the pairing potential for all angles θ. This range is reduced for other orientations, and for $\beta = 0$ it goes to zero, as we can see in figure 3(a). Also a subgap opens within the conductance spectra due to the imaginary s-wave component. Within the subgap in the tunnelling limit, the tunnelling conductance is zero, $\sigma(E) = 0$, while in the metallic limit ($Z = 0$), $\sigma(E) = 2$ independently of the orientation, as in the s-wave case. In the $Z = 0$ case, the normal-reflection coefficient is zero, while the Andreev reflection coefficient is unity. In this case the charge transport into the superconductor is twice as large as in the normal state, for energies within the subgap region.

In the $d_{x^2-y^2} + id_{xy}$ case, seen in figure 4, the tunnelling conductance has residual values within the gap for all orientations β. In particular for $\beta = 0$, as seen in figure 4(a), in the tunnelling limit, the conductance $\sigma(E = 0)$ at $E = 0$ has a non-zero value in contrast to the $(d_{x^2-y^2} + is)$-wave case where it is zero. In the $d_{x^2-y^2} + is$ case for $\beta = 0$, there is no angle θ for which the transmitted quasiparticles experience the sign change of the pair potential, and the tunnelling conductance goes to zero. The situation is different for the $d_{x^2-y^2} + id_{xy}$ case, where for $\beta = 0$ the transmitted quasiparticles feel the sign difference due to the secondary order parameter d_{xy}.

Also, the zero-energy conductance height evolves very differently with the orientation of the superconductor for the three pairing symmetries. This is seen in figure 5 where the dependence of the zero-energy conductance height on β is plotted, for $Z = 2.5$, for the three pairing symmetries. It is seen that for the $(d_{x^2-y^2} + id_{xy})$-wave case (dashed line), for β close to $\pi/4$, the height representing the plateau-like feature seen in figure 4 is enhanced. Also, for angles close to zero, the height of the ZEP for the $(d_{x^2-y^2} + id_{xy})$-wave case is reduced, but is not zero. Note that the height for $\beta = 0$ remains finite even in the large Z-limit, while the height in the $(d_{x^2-y^2} + is)$-wave case goes to zero.

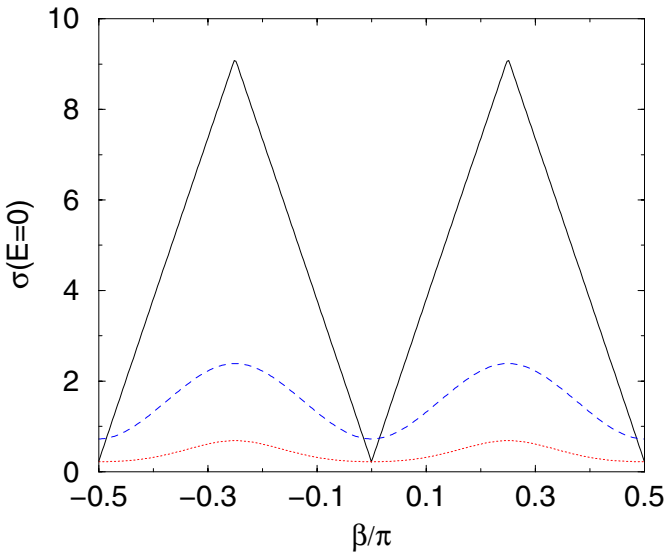

Figure 5. Normalized tunnelling conductance σ for $E = 0$ as a function of β for $Z = 2.5$, and $T = 0$. The pairing symmetry of the superconductor is: $d_{x^2-y^2}$ (solid line), $\Delta_d = 0.7\Delta_0$; $d_{x^2-y^2} + is$ (dotted line), $\Delta_d = 0.7\Delta_0$, $\Delta_s = 0.3\Delta_0$; $d_{x^2-y^2} + id_{xy}$ (dashed line), $\Delta_d = 0.7\Delta_0$, $\Delta_{d_{xy}} = 0.3\Delta_0$.

4. Bound-state energies

These features are explained if we calculate the energy of the mid-gap state, which is given for large Z by the value at which the denominator of equations (7), (8) vanishes. The equation giving the energy peak level is written as [16]

$$\phi_- \phi_+^* n_+ n_-|_{E=E_p} = 1.0. \tag{14}$$

In the $d_{x^2-y^2}$-wave case, for a given angle β, this equation has the solution $E = 0$ for a finite range of angles θ. For $\beta = \pi/4$ the solution is $E = 0$ for $-\pi/2 < \theta < \pi/2$, since $n_+ n_-|_{E=0} = -1$, and also the transmitted quasiparticles feel a different sign of the pair potential, i.e. $\phi_- \phi_+^*|_{E=0} = -1$. In the $(d_{x^2-y^2} + is)$-wave case for $\beta = \pi/4$, the solution is $E = \Delta_s$ in the θ-interval $[0, \pi/2]$. In this case the n_+, n_- and the internal phases are varied in such a way that equation (14) is satisfied for $E = \Delta_s$ and a mid-gap state is formed. When a mid-gap state exists, the tunnelling conductance $\overline{\sigma}_s(E, \theta)$ is equal to 2 for all θ and the peak in $\sigma(E)$ seen in figures 2, 3 is due to the normal-state conductance σ_N in equation (10), which depends inversely on Z^2 for large Z. For intermediate angles β, the peak height of the tunnelling conductance $\sigma(E)$ is proportional to 8β for $0 < \beta < \pi/4$ [3], and for $\beta = 0$ the range of θ-angles for which equation (14) has solutions collapses to zero in both symmetry states, and no bound states are formed. Then $\sigma(E)$ goes to zero as $1/Z^2$ and there is no conductance peak. For energies different to the bound-state energy E_p, for large Z, $\overline{\sigma}_s(E, \theta)$ is inversely proportional to Z^2, as is σ_N, and the tunnelling conductance has a constant value as we can see in figure 2, for $E > 0$. In the $(d_{x^2-y^2} + id_{xy})$-wave case for fixed β, the solutions of (14) depend on both E and θ, as seen in figure 6, where the bound-state energy E_p is plotted for $\beta = 0, \pi/16, \pi/8, \pi/4$, as a function of θ. In this case the mid-gap state for a given β

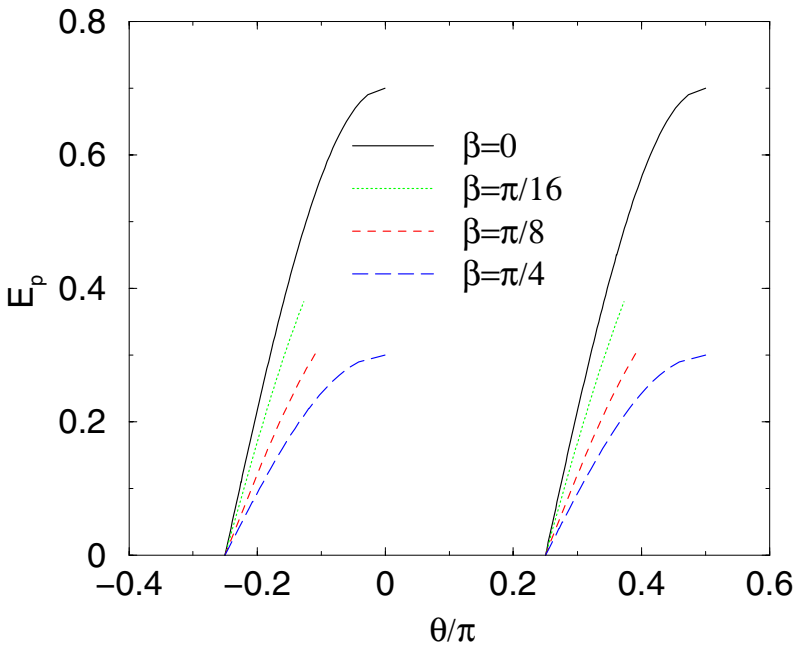

Figure 6. Bound-state energy E_p, for $T = 0$, versus the quasiparticle angle θ for different orientations $\beta = 0, \pi/16, \pi/8, \pi/4$. The pairing symmetry of the superconductor is $d_{x^2-y^2} + id_{xy}$ with $\Delta_d = 0.7\Delta_0$, $\Delta_{d_{xy}} = 0.3\Delta_0$.

is formed for a pair of angles θ, for energies within the gap. This observation can be used to explain the residual values of the tunnelling conductance within the gap, seen in figure 4, as follows. When a bound state is formed, the conductance $\overline{\sigma}_{\rm s}(E,\theta)$ is equal to 2 exactly at the bound-state energy for the two discrete values of θ, and the peak in the $\sigma(E)$ should be proportional to Z^2 for large Z for these values of θ. For the rest of the quasiparticle trajectory angles θ, the tunnelling conductance $\sigma(E)$ has a constant value. Thus the height for a given energy and angle β is determined from the interplay of two competitive factors, i.e. the bound-state energy formed at a couple of θ-angles, which gives a contribution proportional to Z^2, and that for the rest of the θ-angles, which gives a constant-value contribution independent of Z. Also the steps in θ when evaluating the integral in equation (9) are very much crucial, since the calculation of the tunnelling conductance has to be performed exactly at the bound-state energy. If this is not the case, then the peak due to the bound states in the tunnelling conductance would have a smaller value which would depend on Z in general. We conclude that in the $\mathrm{d}_{x^2-y^2}+\mathrm{id}_{xy}$ case the discrete values of the quasiparticle trajectory angle θ for which a bound state is formed compared to the interval of θ-angles in the other two pairing states explains the reduced height of the tunnelling conductance within the gap. However, if we calculate the conductance $\overline{\sigma}_{\rm s}(E,\theta)$ for the $\mathrm{d}_{x^2-y^2}+\mathrm{id}_{xy}$ case at a given β for a value of θ for which a bound state occurs, then the conductance should develop a peak at the bound-state energy, where $\overline{\sigma}_{\rm s}(E,\theta)$ is equal to 2. For the rest of the energies, $\overline{\sigma}_{\rm s}(E,\theta)$ goes to zero. This is seen in figure 7 where the conductance $\overline{\sigma}_{\rm s}(E,\theta)$ for $Z=2.5$ is plotted for fixed $\beta=\pi/4$ as a function of the energy E, for different values of the angle $\theta=\pi/4, 3\pi/8, \pi/2$ for which bound states occur. We see that for $\theta=\pi/4$ the peak is at $E=0$. However, as we change the angle θ towards $\pi/2$, the peak level moves from $E=0$ to $E=\Delta_{\mathrm{d}_{xy}}$.

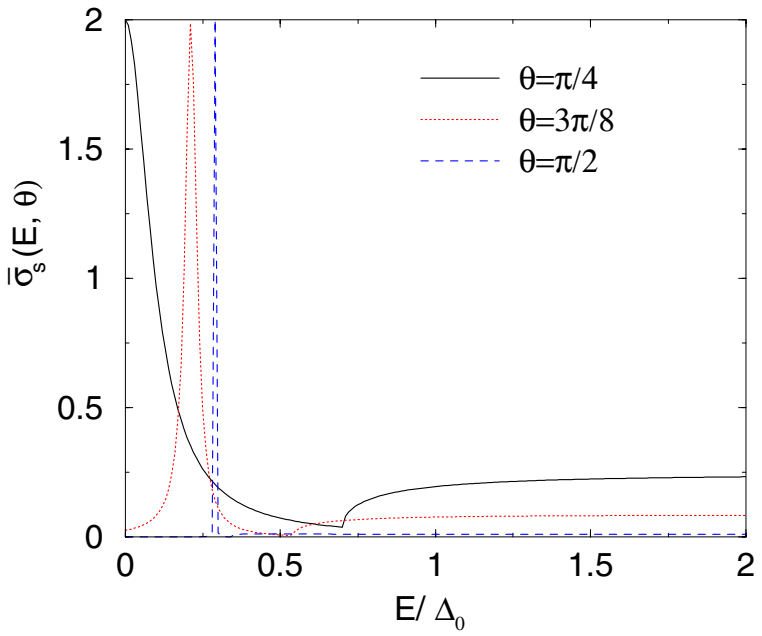

Figure 7. Conductance $\overline{\sigma}_{\rm s}(E,\theta)$ for $Z=2.5$, and $T=0$, as a function of E for fixed angle $\beta=\pi/4$, at different angles $\theta=\pi/4, 3\pi/8, \pi/2$ for which a bound state is formed at a different value of E. The pairing symmetry of the superconductor is $\mathrm{d}_{x^2-y^2}+\mathrm{id}_{xy}$ with $\Delta_{\rm d}=0.7\Delta_0$, $\Delta_{\mathrm{d}_{xy}}=0.3\Delta_0$.

The occurrence of residual density of states in the $(d_{x^2-y^2} + id_{xy})$-wave case is unaffected by the calculation of $\sigma(E)$ including the self-consistency of the order parameter [18]. In this calculation an enhancement appears at $E = \Delta_{d_{xy}}$, for $\beta = \pi/4$. In our calculation we also observed a similar enhancement at $E = \Delta_{d_{xy}}$ when the definition

$$\sigma(E) = \frac{\int_{-\pi/2}^{\pi/2} d\theta \overline{\sigma}_s(E, \theta) \cos\theta}{\int_{-\pi/2}^{\pi/2} d\theta \sigma_N \cos\theta}$$

was used for the calculation of the tunnelling conductance. The $\cos\theta$ factor was included in the integration formula to calculate the x-component of the tunnelling spectra. Within this definition the bound state at $\theta = 0$ contributes more (due to the $\cos\theta$ factor) than the bound state at θ close to $\pi/4$. As seen in figure 6 the bound state at $\theta = 0$ corresponds to energy $E = \Delta_{d_{xy}}$ causing the peak in $\sigma(E)$ at $E = \Delta_{d_{xy}}$. Also in a self consistent calculation the bound state at $(\theta = \pi/4, E = 0)$ contributes less in $\sigma(E)$ than that at $(\theta = 0, E = \Delta_{d_{xy}})$ due to the depletion of the order parameter near the interface. In any case the peak near $E = \Delta_{d_{xy}}$ in $(d_{x^2-y^2} + id_{xy})$-wave pairing state is much more suppressed than that at $E = \Delta_s$ in $(d_{x^2-y^2} + is)$-wave state.

The angular dependence of the bound-state energy for fixed boundary orientation at the xy-plane can be used to identify the $(d_{x^2-y^2} + id_{xy})$-wave pairing state. The method that we propose here is the two-point spectroscopy described by Benistant *et al* [19]. They measured the reflected hole distribution along the boundary y-direction when electrons are injected with a certain distribution $P(\phi)$ through a point contact, at $y = 0$, into a normal metal of thickness d attached to an s-wave superconductor. The presence of a magnetic field parallel to the z-axis deflects the trajectories of the electrons and leads to an asymmetric distribution of angles of incidence in the normal-metal/superconductor interface. Also the magnetic field focuses the reflected holes into a second point contact which acts as a hole collector. Moving the second point contact around the first one or using several point contacts along the direction parallel to the interface, we are able to measure the intensity of the Andreev reflected holes as a function of the y-direction. In the s-wave case one observes a single peak called the 'focusing peak' at $y = y_0$ (with the injection point at $y = 0$), since the Andreev reflected probability amplitudes are independent of the injection angle. For the $(d_{x^2-y^2} + id_{xy})$-wave case, the bound-state energies, for which the reflection coefficient is equal to one, occur at angles $\theta_1 < 0, \theta_2 > 0$ for a given boundary orientation and large barrier strength Z. These bound states will give rise to a second peak in the hole distribution, at a different position, in addition to the one due to the focusing. The presence of the magnetic field leads to an asymmetric distribution of angles of incidence in the interface, and the trajectory which corresponds to the bound state at θ_1 has a shorter path than that at θ_2 and the corresponding injected electrons have smaller angle ϕ. If the angular distribution probability $P(\phi)$ of the injected particles is peaked at small injection angles, this will lead to a contribution to the secondary peak from the bound state at θ_1 larger than that from the bound state at θ_2. This new peak would be observed for all energies for which bound states exist in a $(d_{x^2-y^2} + id_{xy})$-wave superconductor. In the cases of a $d_{x^2-y^2}$-wave superconductor and a $(d_{x^2-y^2} + is)$-wave superconductor, the resonance exists only for $E = 0$ and $E = \Delta_s$ respectively. The magnetic field shifts the bound state spectrum by $\Delta E = \boldsymbol{v}_s \cdot \boldsymbol{k} \sim \sin\theta$ [12], where $\boldsymbol{v}_s$ is the superfluid velocity. Thus, one has to take into account this additional energy shift due to the external field for the correct interpretation of the experimental data. Experiments of this kind require high-quality normal-conducting crystal and point contacts for the electron injection. Any voltage drop has to occur at the point contact for the electrons to move ballistically in the normal metal. A similar procedure has been proposed by Honerkamp and Sigrist [20] for discriminating between unitary and non-unitary triplet states for the superconductor Sr_2RuO_4.

5. Temperature dependence of the tunnelling spectra

At finite temperatures the tunnelling conductance is calculated from the relation [21]

$$\sigma(eV) = \int_{-\infty}^{\infty} \mathrm{d}E \left[-\frac{\partial f(E+eV)}{\partial E} \right] \left(\int_{-\pi/2}^{\pi/2} \mathrm{d}\theta \, \overline{\sigma}_{\mathrm{s}}(E,\theta) \right) \Big/ \left(\int_{-\pi/2}^{\pi/2} \mathrm{d}\theta \, \sigma_N \right). \tag{15}$$

eV is the electron energy and $f(E)$ is the Fermi function $f(E) = 1/(\mathrm{e}^{\beta E} + 1)$, where $\beta = 1/k_B T$. In the case of a two-component order parameter, we assume that below a surface transition temperature a subdominant order parameter can develop which spontaneously breaks the time-reversal symmetry. Its amplitude is below the value for the formation of a state with spontaneously broken time-reversal symmetry in the bulk [12]. The temperature dependence of the pair potential amplitude is assumed to obey the usual BCS relation. As a consequence, under the coexistence of the secondary component, the critical temperatures for the dominant d wave, T_{d}, and the subdominant s (d_{xy}) components, T_{s} ($T_{\mathrm{d}_{xy}}$), directly correspond to the amplitude of the attractive interaction in each case.

Figure 8 shows the tunnelling conductance $\sigma(eV)$ for different temperatures $T/T_{\mathrm{d}} = 0.1, 0.2, 0.3, 0.4$, in the large-barrier-strength limit $Z = 10$, $\beta = \pi/4$. The pairing symmetry of the superconductor is $\mathrm{d}_{x^2-y^2}$-wave symmetry in figure 8(a), ($\mathrm{d}_{x^2-y^2}$+is)-wave symmetry, with $T_{\mathrm{s}} = 0.3T_{\mathrm{d}}$, in figure 8(b), ($\mathrm{d}_{x^2-y^2} + \mathrm{id}_{xy}$)-wave symmetry, with $T_{\mathrm{d}_{xy}} = 0.3T_{\mathrm{d}}$, in figure 8(c). It is seen that due to the thermal occupation of states contributing to the tunnelling current, the peaks are becoming broadened as the temperature increases. In the $\mathrm{d}_{x^2-y^2}$-wave case, as seen in figure 8(a), the ZEP is suppressed when the temperature increases and disappears almost at the critical temperature. This feature of the calculated spectra is consistent with the experimental results for $YBa_2Cu_3O_{7-\delta}$ obtained by low-temperature scanning tunnelling spectroscopy [4]. The evolution of the conductance spectra with temperature is qualitatively similar to that obtained by the calculation including the self-consistency [22]. On the other hand, in the ($\mathrm{d}_{x^2-y^2}$ + is)-wave case, seen in figure 8(b), the tiny subgap of the order of $\Delta_{\mathrm{s}} = 0.3\Delta_0$ at $T = 0$ disappears with the increase of the temperature. For $T > T_{\mathrm{s}}$ it follows the usual $\mathrm{d}_{x^2-y^2}$-wave-like dependence. In the ($\mathrm{d}_{x^2-y^2} + \mathrm{id}_{xy}$)-wave case, shown in figure 8(c), the zero-energy height is suppressed with the increase of the temperature. For $T > T_{\mathrm{d}_{xy}}$ the temperature dependence of the spectra for the ($\mathrm{d}_{x^2-y^2} + \mathrm{id}_{xy}$)-wave state is similar to that for the $\mathrm{d}_{x^2-y^2}$-wave case.

In figure 9 we plot the ZEH as a function of temperature for the three pairing states. For the $\mathrm{d}_{x^2-y^2}$-wave case the ZEH behaves as T^{-1}. For the ($\mathrm{d}_{x^2-y^2}$ + is)-wave case the ZEH increases up to $T = 0.2T_{\mathrm{d}}$ and then decreases with increasing temperature. For $T > T_{\mathrm{s}}$ it follows the $\mathrm{d}_{x^2-y^2}$-wave behaviour. The downturn of the ZEH at low temperatures in the ($\mathrm{d}_{x^2-y^2}$ +is)-wave case accords with the ZEP splitting and has also been observed experimentally (see figure 1 in reference [13]). In the ($\mathrm{d}_{x^2-y^2} + \mathrm{id}_{xy}$)-wave case the ZEH decreases with T on different scales for $T < T_{\mathrm{d}_{xy}}$ and $T > T_{\mathrm{d}_{xy}}$, indicating the different pairing states. In all cases the transition from the $\mathrm{d}_{x^2-y^2}$-wave case to the ($\mathrm{d}_{x^2-y^2}$ +is)-wave case or ($\mathrm{d}_{x^2-y^2}$ +id_{xy})-wave case is continuous.

In the metallic limit ($Z = 0$) (not presented in the figure), the tunnelling conductance at $eV = 0$ decreases, as the temperature increases, from its zero-temperature value $\sigma(eV) = 2$, to the normal-state value $\sigma(eV) = 1$ at the transition temperature. The variation with T for the ($\mathrm{d}_{x^2-y^2}$ +is)-wave case (($\mathrm{d}_{x^2-y^2}$ +id_{xy})-wave case) for $T < T_{\mathrm{s}}$ ($T_{\mathrm{d}_{xy}}$) deviates from the $\mathrm{d}_{x^2-y^2}$-wave behaviour. In both cases where time-reversal symmetry is broken, a change of slope occurs in the $\sigma(eV = 0)$ versus T diagram, at the subdominant-order-parameter transition temperature. However, in this case the variation with T is similar for the $\mathrm{d}_{x^2-y^2}$ + is and $\mathrm{d}_{x^2-y^2} + \mathrm{id}_{xy}$ cases, and thus it cannot be used to discriminate between the two pairing states.

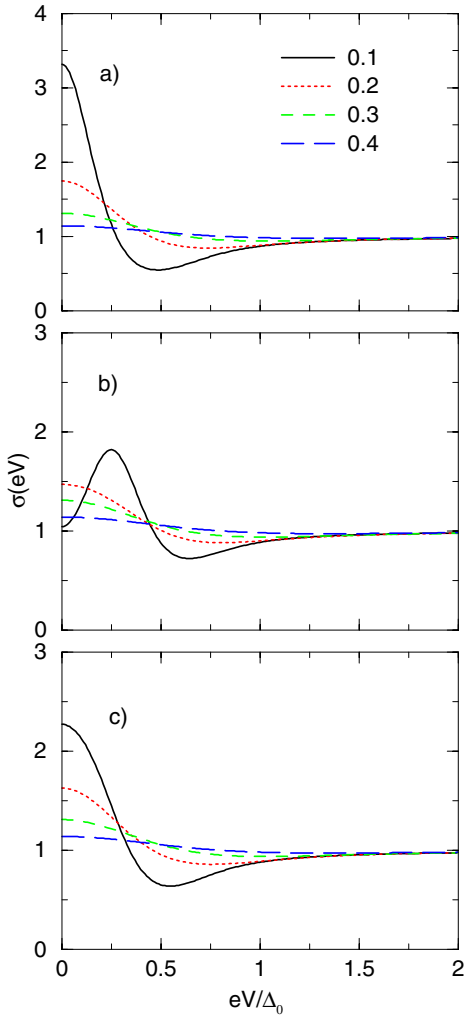

Figure 8. Normalized tunnelling conductance σ versus the applied voltage eV, for different temperatures $T/T_{\rm d} = 0.1, 0.2, 0.3, 0.4$. The barrier strength is $Z = 10$, and the junction orientation is fixed at $\beta = \pi/4$. The pairing symmetry of the superconductor is: $d_{x^2-y^2}$ in (a); $d_{x^2-y^2} + is$ with $T_{\rm s} = 0.3T_{\rm d}$ in (b); $d_{x^2-y^2} + id_{xy}$ with $T_{d_{xy}} = 0.3T_{\rm d}$ in (c).

6. Conclusions

We calculated the tunnelling conductance in normal-metal/insulator/anisotropic superconductors, using the BTK formalism. We showed that the conductance peak for (110) surface orientation, in a $d_{x^2-y^2}$-wave superconductor, appears at zero energy, and is shifted according to the amplitude of the secondary order parameter in the $(d_{x^2-y^2} + is)$-wave case. In the $(d_{x^2-y^2} + id_{xy})$-wave case the tunnelling conductance has residual states within the energy gap. These are due to the formation of bound states at discrete values of the trajectory angle θ for each boundary orientation angle β, for energies within the gap. These bound states explain both the residual states within the subgap and also the small height of the conductance within the subgap region. The calculation of the conductance $\overline{\sigma}_{\rm s}(E, \theta)$ for a given boundary

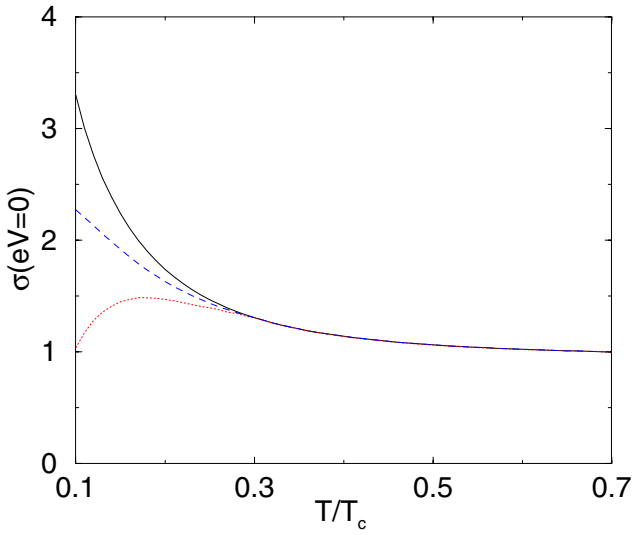

Figure 9. Normalized tunnelling conductance σ for $eV = 0$ as a function of the temperature T/T_{d} for $Z = 10$, and $\beta = \pi/4$. The pairing symmetry of the superconductor is: $\mathrm{d}_{x^2-y^2}$ (solid line); $\mathrm{d}_{x^2-y^2}$ + is with $T_{\mathrm{s}} = 0.3T_{\mathrm{d}}$ (dotted line); $\mathrm{d}_{x^2-y^2} + \mathrm{id}_{xy}$ with $T_{\mathrm{d}_{xy}} = 0.3T_{\mathrm{d}}$ (dashed line).

orientation at an incident angle θ for which a bound state occurs shows an enhancement at the bound-state energy. The dependence of the energy of the bound state on θ can be used within the method of electron focusing to detect the $(\mathrm{d}_{x^2-y^2} + \mathrm{id}_{xy})$-wave state. In such a case, besides the focusing peak, there is another peak in the reflected hole distribution spectrum for all energies of the injected electrons less than the amplitude of the secondary order parameter. This peak should also be observed for the $\mathrm{d}_{x^2-y^2}$-wave and $(\mathrm{d}_{x^2-y^2} + \mathrm{is})$-wave cases, but only at the energies $eV = 0$, $eV = \Delta_s$ respectively.

The zero-energy conductance peak decreases as T^{-1} with increasing temperature and disappears almost at the transition temperature for the $\mathrm{d}_{x^2-y^2}$-wave case. The temperature dependence of the ZEH deviates from the usual T^{-1}-behaviour of the $\mathrm{d}_{x^2-y^2}$ case, in the case where a subdominant surface order parameter is developed, for $T < T_{c1}$, where T_{c1} is the transition temperature for the subdominant order parameter. These features can be used to distinguish between states with broken time-reversal symmetry.

Throughout this paper the spatial variation of the dominant order parameter near the surface, which depends on the boundary orientation, is ignored for simplicity. As a consequence, since the nucleation of the secondary order parameter near the surface depends on the strength of the dominant one, the spatial variation of the secondary order parameter is also ignored. We expect more drastic changes when the orientation is $\beta = \pi/4$, where the suppression of the dominant order parameter is more significant. However, since the features presented here are intrinsic and are generated by the existence of surface bound states, the essential results do not change qualitatively.

Also, we assumed perfectly flat interfaces in the clean limit, so any impurity scattering and the effect of the surface roughness are ignored. Generally, surface roughness will lead to a statistical distribution of the outgoing trajectories, and will alter the results presented. The effect of surface roughness on the tunnelling effect in interfaces between normal metals and superconductors with the time-reversal symmetry broken has been studied previously [23]. It was found that in the $\mathrm{d}_{x^2-y^2} + \mathrm{id}_{xy}$ case, additional bound states are formed due to the

surface roughness. Also, in a $d_{x^2-y^2}$-wave superconductor, the ZEP may appear even for (100) interfaces with surface roughness [12].

Also, in a more realistic treatment of the problem, one has to take into account also the thickness of the barrier. In that case additional resonances are expected in the tunnelling spectra due to multiple Andreev reflections within the barrier, besides the ones due to the bound states.

Acknowledgments

I would like to thank A V Balatsky for discussions and for a careful reading of the manuscript. Also, I wish to thank Yukio Tanaka for providing me with a list of his publications. I received partial support from the ESF programme FERLIN.

References

[1] Blonder G E, Tinkham M and Klapwijk T M 1982 *Phys. Rev.* B **25** 4515
[2] Andreev A F 1964 *Sov. Phys.–JETP* **19** 1228
[3] Tanaka Y and Kashiwaya S 1995 *Phys. Rev. Lett.* **74** 3451
[4] Kashiwaya S, Tanaka Y, Koyanagi M, Talashima H and Kajimura K 1995 *Phys. Rev.* B **51** 1350
[5] Xu J H, Miller J H Jr and Ting C S 1996 *Phys. Rev.* B **53** 3604
[6] Averin D and Bardas A 1995 *Phys. Rev. Lett.* **75** 1831
[7] Hurd M 1997 *Phys. Rev.* B **55** 11 993
[8] Yoshida N, Tanaka Y and Kashiwaya S 1999 *Physica* C **317–318** 666
[9] Ghosh A and Adhikari S K 1998 *Physica* C **309** 251
[10] Ghosh A and Adhikari S K 1999 *Physica* C **322** 37
[11] Matsumoto M and Shiba H 1995 *J. Phys. Soc. Japan* **64** 3384
[12] Fogelstrom M, Rainer D and Sauls J A 1997 *Phys. Rev. Lett.* **79** 281
[13] Covington M, Aprili M, Paraoanu E, Green L H, Xu F, Zhu J and Mirkin C A 1997 *Phys. Rev. Lett.* **79** 277
[14] Aprili M, Badica E and Greene L H 1999 *Phys. Rev. Lett.* **83** 4630
[15] Krupke R and Deutscher G 1999 *Phys. Rev. Lett.* **83** 4634
[16] Kashiwaya S, Tanaka Y, Koyanagi M and Kajimura K 1996 *Phys. Rev.* B **53** 2667
[17] Zhu J-X and Ting C S 1998 *Phys. Rev.* B **57** 3038
[18] Tanaka Y, Tanuma Y and S Kashiwaya 2001 preprint cond-mat/0101277
[19] Benistant P A M, van Kempen H and Wyder P 1983 *Phys. Rev. Lett.* **51** 817
[20] Honerkamph C and Sigrist M 1998 *J. Low Temp. Phys.* **111** 898
[21] Tinkham M 1996 *Introduction to Superconductivity* (New York: McGraw-Hill)
[22] Barash Yu S, Svidzinsky A A and Burkhardt H 1997 *Phys. Rev.* B **55** 15 282
[23] Rainer D, Burkhardt H, Fogelstrom M and Sauls J A 1998 *J. Phys. Chem. Solids* **59** 2040